

A Real-Time Testbed for Satellite and Terrestrial Communications Experimentation and Development

K. Angkasa, J. Hamkins, J. Jao, N. Lay, E. Satorius, A. Zevallos
Jet Propulsion Laboratory, California Institute of Technology,
4800 Oak Grove Drive, Pasadena, California 91109

Abstract

This paper describes a programmable DSP-based testbed that is employed in the development and evaluation of blind demodulation algorithms to be used in wireless satellite or terrestrial communications systems. The testbed employs a graphical user interface (GUI) to provide independent, real-time control of modulator, channel and demodulator parameters and also affords real-time observation of various diagnostic signals such as carrier, timing recovery and decoder metrics. This interactive flexibility enables an operator to tailor the testbed parameters and environment to investigate the performance of any arbitrary communications system and channel model. Furthermore, a variety of digital and analog interfaces allow the testbed to be used either as a stand-alone digital modulator or receiver, thereby extending its experimental utility from the laboratory to the field.

1 Introduction

Blind demodulation of communication signals under a variety of unknown channel conditions is an area of significant and active interest for both terrestrial and satellite based applications. The testbed described in this paper has been designed to facilitate the development, comparison and evaluation of novel detection techniques. The testbed system comprises integrated hardware and software components that may be operated in both real- and non-real-time. Digital signal processors (DSP'S) coupled with a general purpose processing unit provide for algorithm implementation and user interface and control. In Figure 1, a functional block diagram of the testbed shows the details of the test signal generation and demodulation functions that are divided between three blocks: the modulator, channel, and demodulator blocks. A graphical user interface (GUI) enables user operation and control of the testbed.

The testbed is targeted towards the development of algorithms that facilitate the demodulation of communications signals that have been distorted by a variety of channel impairments. These distortions include intersymbol interference (static and time-varying with uncorrelated taps), additive Gaussian noise, additive coherent interference (e.g. CW or modulated signals) and time-varying carrier phase.

The paper is organized into two sections consisting of an architectural description and a description of various blind demodulation tests and the corresponding performance results for analog and digital modulations. In the testbed architecture section, both the hardware and software design of the testbed and its intended use within the overall context of an algorithm development methodology are discussed in detail. In addition, baseline capabilities are reviewed including generic digital modulators and demodulators for M-ary PSK, M-ary QAM and similar complex signal formats, blind and decision directed linear equalizers, and blind maximum likelihood based data sequence estimators.

The performance results section provides both algorithmic description and quantitative performance results for different blind equalization techniques. As an example, we describe the O_s^r Rectangular method which has been specifically designed to equalize high order QAM constellations while providing a low residual ISI. Performance results are compared to more conventional techniques such as the constant modulus algorithm. Blind demodulation performance of signals distorted by a spectral null channel are also examined in terms of linear versus maximum likelihood sequence estimation techniques.

2 System Architecture

The real-time communications testbed has been developed for a number of interrelated purposes. It is primarily a platform upon which to test new demodulation algorithms against controlled data and against a "library" of existing techniques. The goal being a fair evaluation to demonstrate improvement

or loss compared to conventional approaches. A secondary purpose is to impose a certain level of practicality upon the algorithm development process by attempting to achieve real-time implementations for narrowband signal demodulators. Furthermore, testbed algorithm implementation is only performed with promising candidate techniques that meet a dual requirement of performance improvement and moderate complexity.

2.1 System Hardware and Software

The communications testbed hardware is composed of different programmable processing elements that implement both control of the testbed and the signal processing algorithms employed for demodulation. By selecting hardware components from commercially available VME-bus board level products, a fairly rapid system integration can be achieved. The elements that implement GUI and system control consist of a Motorola 68040 processor board and a corresponding X-Windows server. The software developed for the GUI and system operation reside in a real-time operating system environment (VX-Works) which enables automated scheduling of various system processes. Some of these processes include remote operation and user displays as well as real-time storage of demodulator parameters and decoded data. An example screen of the GUI is shown in Figure 2.

The graphical user interface of the testbed is designed using XDesigner of the Imperial Software Technology. XDesigner is an interactive tool for building GUIs using widgets of the standard OSF/Motif toolkit as building blocks. The designed GUI is then compiled and sits on a real-time operating system which allows multiple tasks to be running simultaneously with priorities given to the more critical tasks.

Consequently, results of such tasks can be displayed using laboratory's signal analyzers and/or any terminal which handles X. The latter was made possible through an integration with SciPlot Widget of the Free Software Foundation, Inc., a widget capable of plotting Cartesian or polar graphs, including logarithmic axes in Cartesian plots. This widget is subclasses directly from the Core widget class and may be freely used with Athena, Motif or the Open Look/Xview widget sets. These plots enable real-time monitoring of the transmitted, distorted or equalized signal quality via constellation plots, for example.

On the signal processing side, the hardware consists of TMS320C40 floating point DSP boards.

In addition, low rate (< 200 kHz) dual channel A/D and D/A's allow analog I/O of complex baseband waveforms as shown in Figures 3 and 4 representing respectively, a **multipath** distorted 8PSK waveform and a blindly equalized version. This output signal capability coupled with the X-Windows based real-time plots affords the user a good level of flexibility in evaluating system and receiver performance. Furthermore, by developing the DSP software in C, we are able to achieve fairly rapid prototyping of real-time demodulators. In addition to the programmable signal processor hardware, digital demodulation from a more typical IF (e.g. 10.7 or 21.4 MHz) is achieved through the use of a high speed 10 bit 65 MHz A/D coupled with a complex downconverter board. The downconverter employed within the testbed is capable of demodulating up to eight medium bandwidth channels in parallel and then interfacing directly to the serial ports of the C40 DSP'S.

2.2 System Functionality

In order to develop demodulation techniques under varying channel conditions, a controlled channel simulation environment has been established in conjunction with the associated modulators and demodulators (modems). From the point and click GUI, the user is at liberty to select transmitter parameters **such** as the complex modulation type and desired spectral shaping. Channel selections correspond to such impairments as **bandlimiting**, finite-impulse-response (FIR) **multipath**, additive noise and carrier frequency offsets. Control of both the signal generation and channel blocks allow for well-calibrated evaluation of the performance of the different demodulators. Both modulated and unmodulated co-channel interference may also be synthesized. For digital signal demodulation, fixed or adaptive equalizers can be selected -- either for benchmark or test purposes with a "menu" allowing the modification of various real-time parameters including data and sampling rate and internal or external signal interfaces.

3 Blind Demodulator Testing

In this section, we discuss different areas of investigation for which the testbed is employed. These areas are currently subdivided between techniques that address interference suppression and/or cancellation for analog modulations (e.g. FM, AM, SSB) and algorithms that provide solutions to

blind demodulation of digitally bauded signals in the presence of frequency selective fading.

3.1 Interference Suppression Tests

The first suite of testbed implemented interference cancellation applications concentrated on the use of cross-coupled phase locked loop designs [1-3] to mitigate CW and modulated interference upon FM signals. While these implementations proved fruitful for demodulating narrowband FM in an additive CW environment, modulated interferers produced significantly worse performance. The testbed has since been employed in comparative testing of other systems such as the amplitude locked loop [4] and is currently being programmed with a trellis based phase detection technique [5].

3.2 Blind Adaptive Equalizers

Among the more robust methods that also exhibit fairly low processing complexities are the time recursive formulations of CMA, a modulus restoral technique [6], and a **cumulant-based signal restoral** approach [7]. These blind equalizers represent baseline approaches for the purposes of performance comparison. These and others under development demonstrate an insensitivity to frequency offsets which allows equalization without full carrier recovery. A new class of cost functions was derived in [9], which extended the real-valued, variable norm cost function, originally developed for geophysical **deconvolution**, to blind complex equalization. One example from this class that is particularly suited for high order square constellations is the $O_{s,RECT}^r$ cost function (1) and (2). The variables r and s are algorithm parameters that control the adaptation properties (typically, $t=2$, $s \gg r$).

$$O_{s,RECT}^r = \frac{\left\{ \frac{1}{N} \sum_{k=1}^N |z_k|^r \right\}^{1/r}}{\left\{ \frac{1}{N} \sum_{k=1}^N \left(|\Re(z_k)|^s + |\Im(z_k)|^s \right) \right\}^{1/s}} \quad (1)$$

$$O_{s,RECT}^r \xrightarrow{s \rightarrow \infty} \frac{\left\{ \frac{1}{N} \sum_{k=1}^N |z_k|^r \right\}^{1/r}}{\max \left\{ |\Re(z_i)|, |\Im(z_i)| \right\}_{i=1}^N} \quad (2)$$

In (1) and (2), z_n denotes the complex equalizer output time samples and N represents a batch sample

block size. The maximization of this cost function yields blind signal recovery and a measure of phase coherency. For real-time implementation, we have developed a time-recursive form (3), where \mathbf{w}_n represents the linear equalizer weight vector and \mathbf{r}_n corresponds to the elements of the equalizer tapped delay line.

$$\mathbf{w}_{n+1} = \mathbf{w}_n - \mu \left\{ \Re(z_n) \cdot |\Re(z_n)|^{s-2} + i \cdot \Im(z_n) \cdot |\Im(z_n)|^{s-2} - R_{O_{s,RECT}} z_n \right\} \mathbf{r}_n^* \quad (3)$$

Real-time demodulator results for both 64- and 256-QAM constellations are shown in Figures 6-7 and 8-9, respectively. Figure 5 details the equalizer-demodulator configuration utilized in conjunction with the $O_{s,RECT}^r$ algorithm. Unlike more standard approaches [8], the PLL is positioned prior to equalizer as the greatest performance improvement achieved by the new algorithm occurs in the low frequency offset regime. In Figure 6 and 8, the mean square demodulator error is plotted for CMA, SW and $O_{s,RECT}$ equalizers. A significantly lower MSE is achieved by the new algorithm, but at the cost of convergence time. To investigate this behavior, the new equalizer was re-evaluated with an increased step size resulting in the performance plots of Figures 7 and 9. Significant improvement is still demonstrated over the conventional equalizers in both acquisition time and residual demodulator error.

3.3 Blind MLSE Demodulators

In order to treat the problem of data detection in the presence of spectral null channels, a joint channel and data sequence estimator was implemented in the testbed using the PSP algorithm [10]. Generically, an MLSE receiver attempts to minimize the Euclidean distance between the observed signal vector and data symbols convolved with an estimated channel (4). The surviving data sequence selection is mechanized through the use of the Viterbi algorithm. For PSP, the channel estimates are updated recursively, *for each state*, according to (5), where $\mathbf{h}(\mathbf{u})$ represents the channel estimate vector associated with each state and β is an adaptation rate step size.

$$\min_{\hat{\mathbf{a}}_N} |\mathbf{r}_N - \hat{\mathbf{H}}(\mathbf{r}_N, \hat{\mathbf{a}}_N) \cdot \hat{\mathbf{a}}_N|$$

where, $\mathbf{r}_N \equiv$ observations, $\hat{\mathbf{H}} \equiv$ channel estimates,
 $\hat{\mathbf{a}}_N \equiv$ data estimates

(4)

$$\hat{\mathbf{h}}(\mu_k) = \hat{\mathbf{h}}(\mu_{k-1}) + \beta \cdot \varepsilon(\mu_{k-1} \rightarrow \mu_k) \cdot \hat{\mathbf{a}}^*(\mu_{k-1} \rightarrow \mu_k)$$

where, $\varepsilon(\mu_{k-1} \rightarrow \mu_k) = r_k - \hat{\mathbf{h}}(\mu_{k-1}) \cdot \hat{\mathbf{a}}(\mu_{k-1} \rightarrow \mu_k)$

(5)

Quantitative test results are shown in Figures 10 and 11 that compare data detection performance for linear equalizers and a blind data sequence estimator. The modulation type is QPSK with 100% root Nyquist pulse shaping transmitted at a symbol rate of 5 kHz and passed through a two equal tap spectral null channel. In Figure 10, the steady-state (after convergence) equalizer and symbol-by-symbol detector error rate is shown as a function of SNR. In Figure 11, different ensemble averaged acquisition curves are shown for four different SNR'S. The first point to note is that the blind linear equalizer convergence time was observed to be 5 to 10 times that of the PSP demodulator – even with PSP channel estimates initialized to zero. If the detection performance is also compared, for an 8 dB SNR, the detected symbol error rate is one to two orders of magnitude better.

4 Conclusions

A real-time, digitally based testbed has been developed for evaluating demodulation algorithms in communications systems. In addition to serving as a prototyping tool for algorithm implementation, its integrated design affords the user an unbiased capability in the evaluation of new receiver designs and demodulation techniques.

5 References

[1] F. Cassara, H. Schachter, G. Simowitz, "Acquisition Behavior of the Cross-Coupled Phase-Locked Loop FM Demodulator," *IEEE Trans. Comm.*, v. COM-28, pp. 897-904, 1980.

[2] Y. Bar-ness, F. Cassara, H. Schachter, R. DiFazio, "Cross-Coupled PLL Interference Canceller with Closed Loop Amplitude Control," *IEEE Trans. Comm.*, v. COM-32, pp. 195-199, 1984.

[3] G. Zimmerman, "Applications of Frequency Modulation Interference Cancelers to Multiaccess Communications Systems," Ph. D. dissertation, California Institute of Technology, Pasadena, CA, 1990.

[4] A. Pettigrew et al., "Test Results for the Ampsys FM-201/5 High Performance Demodulator," Product Notes, Ampsys Laboratories, University of Paisley, Paisley, Scotland.

[5] J. Hamkins et al., "A Comparative Study of Co-Channel Interference Suppression Techniques," *International Mobile Satellite Conference (IMSC '97)*, Pasadena, CA, 1997.

[6] D. Godard, "Self-Recovering Equalization and Carrier Tracking in Two-Dimensional Data Communication Systems," *IEEE Trans. On Comm.*, Vol. COM-28 No. 11, pp. 1867-1875, November 1980.

[7] O. Shalvi and E. Weinstein, "New Criteria for Blind Deconvolution of Nonminimum Phase Systems (Channels)," *IEEE Trans. on Info. Theory*, Vol. 36 No. 2, pp. 312-321, March 1990.

[8] N. Jablon, "Joint Blind Equalization, Carrier Recover, and Timing Recovery for High-Order QAM Signal Constellations," *IEEE Trans. Sig. Proc.*, Vol. 40, pp. 1383-1398, June 1992.

[9] E. Satorius and J. Mulligan, "An Alternative Methodology for Blind Equalization," *Digital Signal Processing*, Vol. 3, pp. 199-209, July 1993.

[10] R. Raheli, A. Polydoros, C. Tzou, "The Principle of Per-Survivor Processing: A General Approach to Approximate and Adaptive MLSE," *IEEE Trans. on Comm.*, Vol. 43 Nos. 2-4 Part 1, pp. 354-364, February-April 1995.

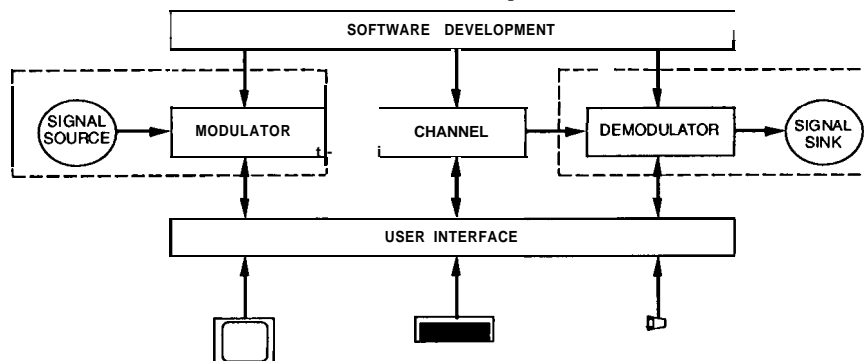


Figure 1. Testbed Functional Block Diagram

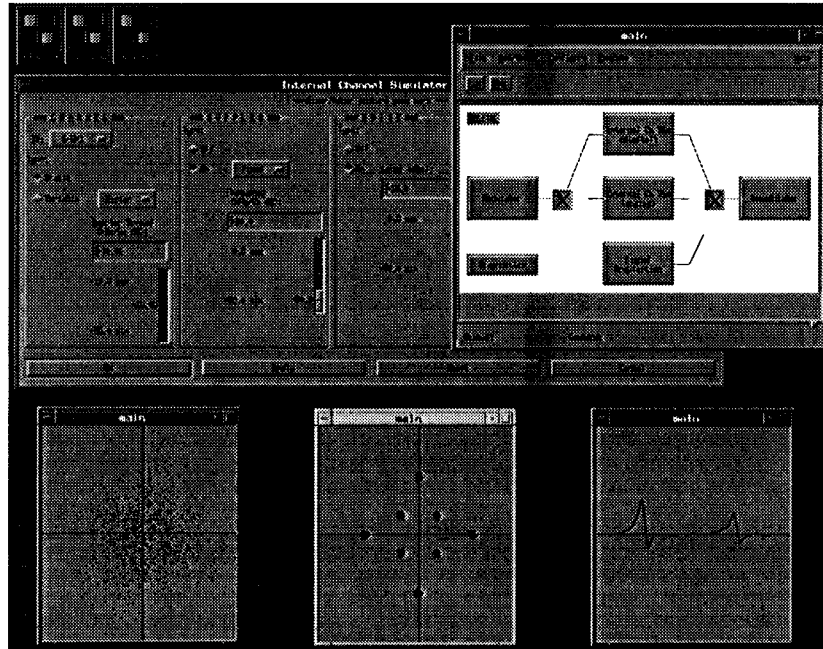


Figure 2. Motif/X-Windows Based Graphical User Interface

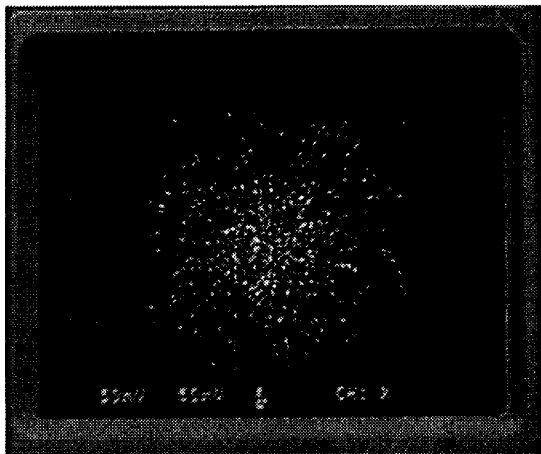


Figure 3. Multipath Distorted 8PSK Signal

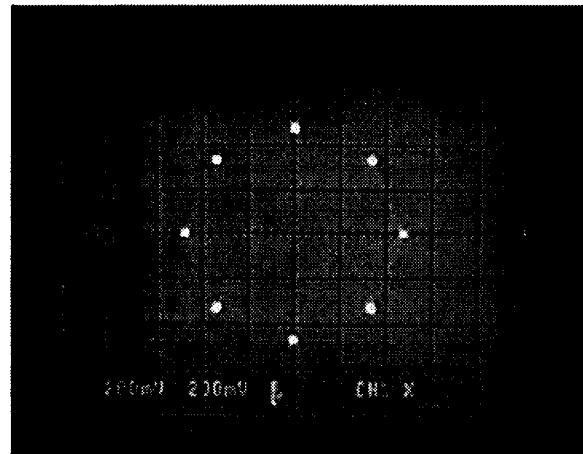


Figure 4. Recovered /Equalized 8PSK Constellation

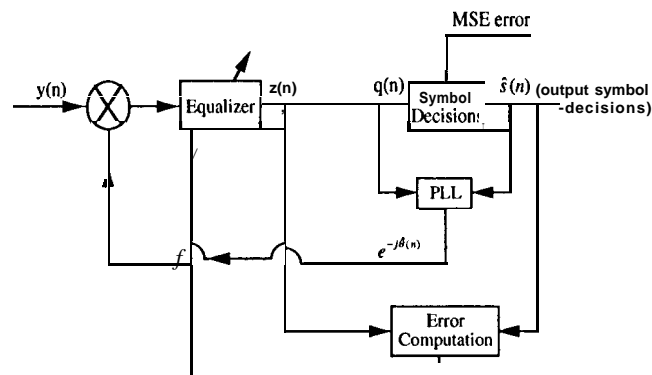


Figure 5. O-rs RECTBlind Equalizer Configuration

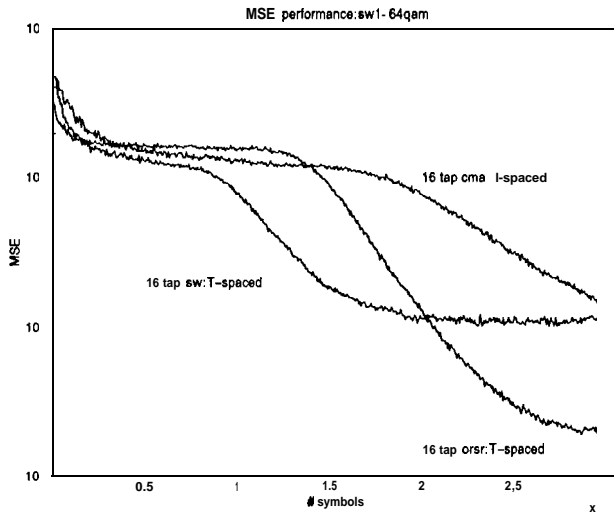


Figure 6. 64-QAM Ors-RECT vs. CMA/SW

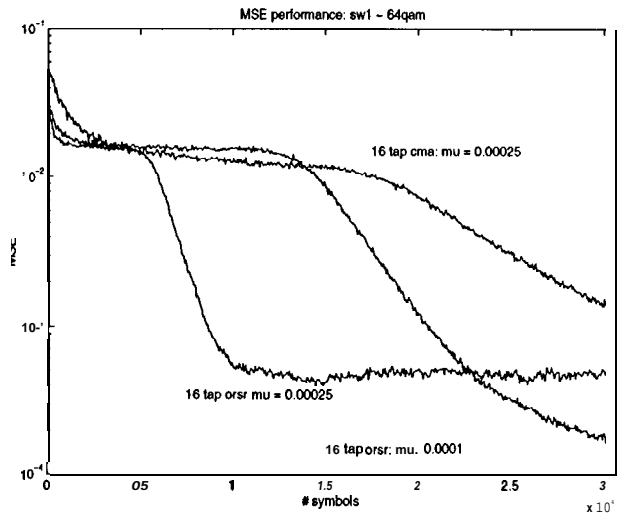


Figure 7. 64-QAM Ors-RECT Varying Step Sizes

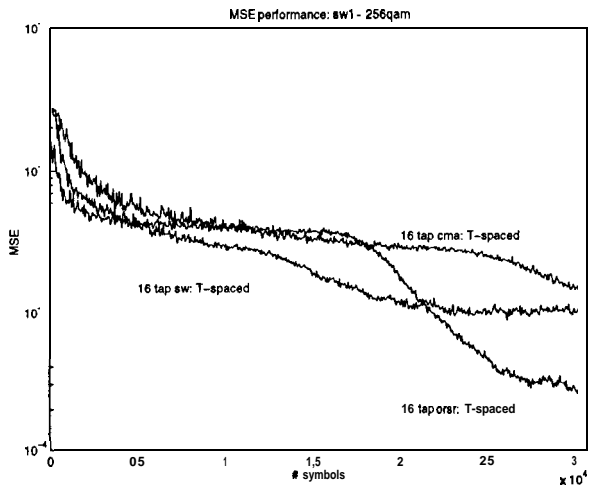


Figure 8. 256-QAM Ors-RECT vs. CMA/SW

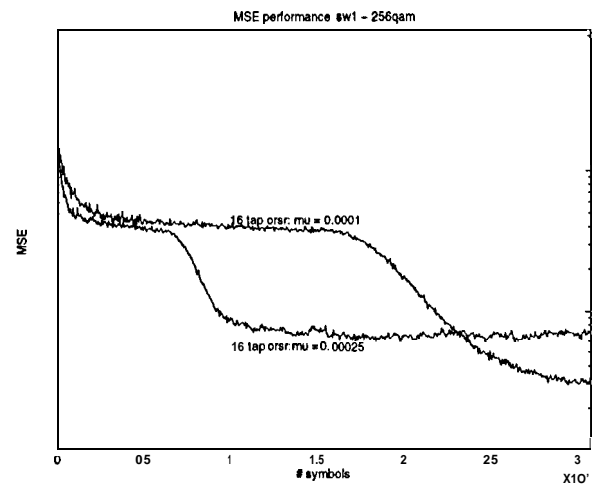


Figure 9. 256-QAM Ors-RECT Varying Step Sizes

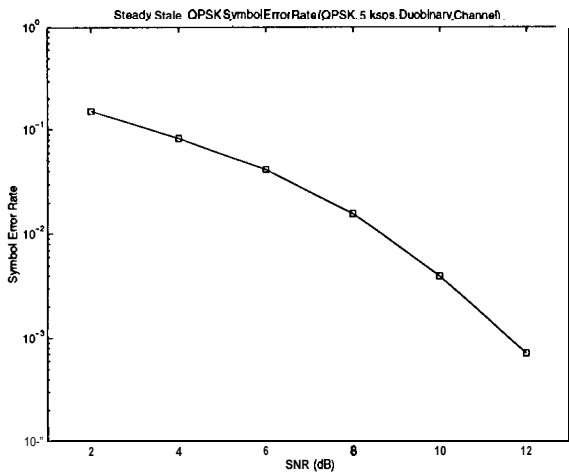


Figure 10. QPSK Linear Equalizer Performance

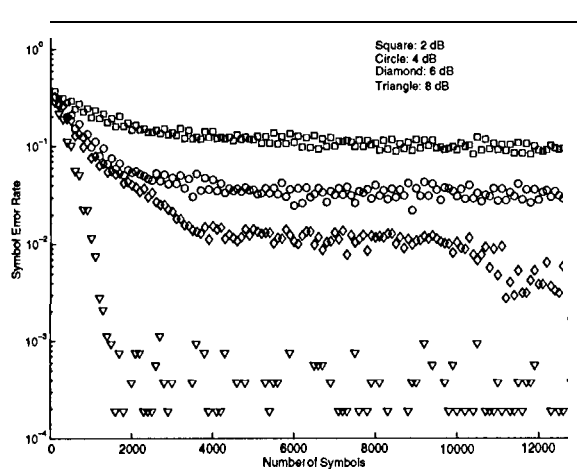


Figure 11. QPSK PSP Acquisition Performance